Zero-knowledge Real-time Indoor Tracking via Outdoor Wireless Directional Antennas

Thadpong Pongthawornkamol, Shameem Ahmed, Klara Nahrstedt
University of Illinois at Urbana-Champaign, USA
{*tpongth2,ahmed9,klara*}*@cs.illinois.edu*

Akira Uchiyama
Osaka University, Japan
utiyama@ist.osaka-u.ac.jp

***Abstract*—WiFi localization and tracking of indoor moving objects is an important problem in many contexts of ubiquitous buildings, first responder environments, and others. Previous approaches in WiFi-based indoor localization and tracking either assume prior knowledge of indoor environment or assume many data samples from location-fixed WiFi sources (i.e. anchor points). However, such assumptions are not always true, especially in emergency scenarios. This paper explores the possibility of real-time indoor localization and tracking *without* any knowledge of indoor environment and with real-time data samples from only few anchor points *outside* the building. By using a small set of synchronized directional antennas as outdoor anchor points to actively scan in various directions, a moving device inside the building can be localized and tracked from the received signal in real-time manner. The paper proposes an angle-of-arrival estimator for accurate localization and adaptive per-antenna angular scheduling for real-time indoor tracking. The validation results from real experiment and simulation yield effectiveness and accuracy of the proposed schemes.**

I. Introduction

Identifying the position and movement of a mobile device in indoor environment is one of very fundamental yet currently active research problems in pervasive and ubiquitous computing, as it is a building block for many context-aware applications. While a Global Positioning System (GPS) device can be used to locate and track a mobile object in outdoor environment, its sky-visibility requirement prevents its use in indoor environment. Hence, other types of medium have been proposed to be used in indoor localization and tracking instead [1]–[5]. Among such media, wireless radio (WiFi) has become one of preferred candidates to localize and track objects indoor due to its widespread usage and non-intrusive nature to human.

Over the past few years, there has been a significant amount of work in WiFi-based indoor localization and tracking [1], [2], [6]–[8]. These wifi-based indoor localization and tracking techniques can be divided into two categories. The first category is the use of omni-directional WiFi signal with WiFi signal strength as the location indicator [1], [2]. To achieve good accuracy, this class of approaches requires the knowledge of building environment (i.e. building layout, signal propagation model, signal fingerprint map) to be known. The second category of Wifi-based localization and tracking is the use of directional WiFi signal with signal strength to estimate the *angle-of-arrival (AOA)* and distance between each anchor and the client [6]–[8]. This class of approaches assumes multiple directional antennas with fixed locations (i.e. anchors) to collect large amount of reading samples over time to get good accuracy. However, the assumptions made by both approaches might not be true in many scenarios, especially in *emergency scenarios* such as fire-fighting situations and disaster-recovery missions, which have the following constraints and characteristics:

No supporting infrastructure: As emergency events could take place anywhere at anytime, the indoor localization algorithm cannot assume support from any existing infrastructure and the background knowledge of the buildings. Even though the background knowledge of the building is available, it may not be accurate at the time of the operation due to the possibility of sudden change in the environment characteristics (i.e. high temperature level, collapsing walls). Hence, the localization and tracking algorithm must rely on external outdoor equipments and on-the-fly, spontaneously-generated information on the spot of the operation.

Few data samples from few outdoor-only anchors: The localization system must be set up in a very short time in any possible terrain. Hence, the localization system cannot assume more than a few external anchors that can be set up and calibrated quickly (e.g., within a couple of minutes). Moreover, since a target in these scenarios usually moves constantly, it is not possible to get a complete coverage of data samples for any specific location. Hence, the localization and tracking algorithm must take into account client mobility and stale data samples in locating the target.

High accuracy and quick response: The localization system must locate and track the device with the highest granularity as possible (e.g., less than few meters error) with limited amount of signal samples and, at the same time, return the answer to the control unit as soon as possible (e.g., millisecond-scale computation and communication delay).

To address such requirements, this paper presents a novel indoor localization and tracking by using a small set of outdoor directional antennas that are deployed on-the-fly outside the building (e.g. in emergency vehicles or firefighter trucks). In contrast to omni-directional antennas, directional antennas provide strong signal in one direction. Hence, it is possible for strong and focused signal strength from directional antennas to penetrate through building walls.

The basic concept of the localization with directional

978-1-4244-5328-3/09/$25.00 ©2009 IEEE

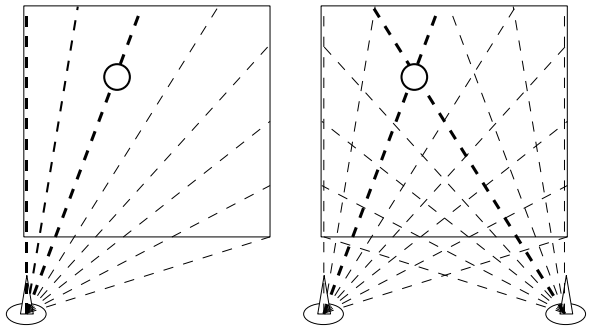

(a) Angle of Arrival (b) Intersecting Lines

Figure 1. Positioning Based on Angle-of-Arrival (AoA)

antennas is as follows. Each antenna periodically rotates in different angles, but with a schedule known to the control unit (e.g. the commander of the operation). The mobile device, in turn, passively measures the signal strength between itself and each of the antennas and reports the values back to the control unit via wireless communication. Based on the measured signal strength values and the antennas' schedules, the control unit can predict the angle-of-arrival (AoA) between the target and each of the antennas (i.e. Figure 1(a)). Given the known geographical coordinates of multiple antennas and the AoA values, the target's position then can be identified by intersecting AoA line from each antenna altogether, as illustrated in Figure 1(b). Furthermore, the estimated location of the mobile device can help the control unit to adjust the scan schedule of each antenna for better tracking granularity and accuracy.

While the use of predicted AoA of directional antennas to localize the client has already been presented in the literature [6]–[8], this paper has several novel contributions. First, this paper discusses the use of outdoor antennas to localize and track indoor targets, where the AoA prediction can be much more affected by outdoor noise and building walls with low signal penetration. Second, this work assumes stale data samples collected from a relatively smaller set of outdoor anchors compared to other works, representing more realistic emergency scenarios. Finally, the paper presents the adaptive antenna scheduling for the real-time tracking of indoor mobile devices. To the best of our knowledge, this is the first work to explore the use of external directional antennas for real-time tracking of indoor mobile objects in emergency scenarios.

This paper has the following organization. Section II discusses the system model and assumptions in the real-time outdoor-to-indoor tracking problem. Section III then presents a novel algorithm to estimate the angle-of-arrival and distance between each directional antenna and the client. Section IV then proposes the adaptive directional antenna scheduling algorithm based on the location feedback from the mobile device. Section V then presents the validation results based on a combination of hand-on experiments and simulations. Section VI then discusses related works in WiFi-based indoor localization and tracking. Finally, Section VII concludes the paper.

II. Model and Assumptions

This section presents the problem setting along with assumptions made by this work.

A. Real-time Indoor Localization and Tracking

The objective of the paper is to track a moving object inside a building by using a small set of directional antennas deployed outside the building. Specifically, for a moving device inside the building, the objective is to find the geographical coordinate (i.e. a latitude-longitude value pair) of the device. In this work, we omit the height information and assume 2-dimensional tracking. However, our approach can also be used for 3-dimensional tracking if the antennas can be rotated in vertical angles. In this paper, we use the terms anchor and antenna interchangeably.

We assume the deployment positions of directional antennas to be given by the geographical constraints, which vary according to each scenario. However, we assume the number of deployed directional antennas to be more than one, but very few (i.e. 2-4 antennas). We assume the geographical coordinates $l_{a_i} = (x_{a_i}, y_{a_i})$ of each antenna a_i to be known by either outdoor positioning systems (e.g., GPS devices) or landmark-to-coordinate mapping via satellite image services (e.g., Google Maps [9]). The angle calibration of each antenna is assumed to be done with the use of a magnetic compass. Lastly, our proposed tracking algorithm assumes a real-time communication channel such as a wireless link between the mobile device and the control unit for the target to report back the collected sample to the control unit, so that the control unit can localize and track the target.

B. Hardware Assumptions and Target Mobility Model

In addition to the antenna location information, we assume the following information to be known.

Antenna angle space: the available direction list, denoted by $\Theta_i = [\theta_{i0}, \theta_{i1}, ..., \theta_{i\{n_i-1\}}]$, consists of all global angle values relative to the magnetic north pole that the antenna a_i can point to, where n_i denotes the total number of available directions of antenna a_i. The parameters Θ_i and n_i are based on hardware capability and calibration of the antenna.

Signal reading latency: the signal reading latency, denoted by d_i, represents the delay for a receiver to collect one reading sample from the antenna a_i after a_i switches to its current direction. The latency d_i includes the time for the directional antenna to switch angle and the time for the receiver to collect a reading sample that represents the current antenna angle. This value, also, depends on the angular speed of the antenna and the precision of the mobile device. In practice, the value d_i can range from ten milliseconds to several hundred milliseconds or even a few seconds. This value play an important role of the tracking performance, as we will see in Section V.

Target speed: We assume the target's maximum speed, denoted by V_{max} to be known. This value could range over few meters per second, as it represents the possible range of human speed when moving inside the building.

III. Static Localization Algorithm

In this section, we present a novel location estimation algorithm of a target based on its currently observed signal strength from each angle of each antenna. That is, from each antenna a_i, a signal strength vector $S_i = [s_{i0}, s_{i1}, s_{i2}, ... s_{i\{n_i-1\}}]$ is given, where s_{ik} is the received signal strength indicator (RSSI) from antenna a_i at direction $\theta_{ik} \in \Theta_i$ to the target device. Given S_i from each a_i, the algorithm estimates the location $l^* = (x^*, y^*)$ of the target. This algorithm does not consider stale reading due to the target's movement over time. Such tracking problem will be addressed by the algorithm in Section IV.

This section first presents the generic probabilistic, grid-based localization in Section III-A. The two schemes of probability estimation based on the observed signal strength from each angle are then presented in Section III-B. Finally, some additional techniques for better estimation are proposed in Section III-C.

A. Probabilistic, Grid-based Localization Framework

Our localization algorithm uses the probabilistic, grid-based approach as follows. The entire target's possible location is divided into several small square areas of equal size called *cells*. Let N be the number of total cells and $l_{c_j} = (x_{c_j}, y_{c_j})$ be the location of the center of cell c_j, where $1 \leq j \leq N$. For each cell c_j and the signal strength vector S_i from antenna a_i, we estimate the probability p_{ji}, which is the probability that the target is located at cell c_j given the signal reading from the antenna a_i. That is,

$$p_{ji} = P[l^* = l_{c_j} | S_i]$$

In the Section III-B, we will discuss the estimation of p_{ji}.

If there are M antennas in the system, we define a signal strength matrix $S = [S_1, S_2, .., S_M]$ as the reading values from all angles of all antennas in the system. Assuming each antenna is independent from each other , we can calculate $p_j = P[l^* = l_{c_j}|S]$, which is the probability that the target's location is in cell c_j given the signal matrix S, as

$$p_j = \alpha . \Pi_{i=1}^{M} p_{ji} \quad (1)$$

, where α is the normalizing factor that makes the total probability equal to 1.

Hence, given an appropriate estimator of p_{ji} and signal matrix S, we can calculate the probability distribution of the client's location in each cell. The estimated target's location $l^* = (x^*, y^*)$ is then calculated as the weighted centroid of the location center of each cell. That is,

$$x^* = \Sigma_{j=1}^{N} p_j . x_{c_j}$$

and

$$y^* = \Sigma_{j=1}^{N} p_j . y_{c_j}$$

Also, we mathematically define the angle-of-arrival from location $l_{\text{from}} = (x_{\text{from}}, y_{\text{from}})$ to location $l_{\text{to}} = (x_{\text{to}}, y_{\text{to}})$, denoted by $\theta(l_{\text{from}}, l_{\text{to}})$, as

$$\theta(l_{\text{from}}, l_{\text{to}}) = \arctan(\frac{y_{\text{to}} - y_{\text{from}}}{x_{\text{to}} - x_{\text{from}}}) \quad (2)$$

In the next subsection, the paper will discuss the estimator functions of per-cell, per-antenna probability p_{ji} based on per-antenna signal strength vector S_i.

B. Per-anchor Location Probability Estimation

As mentioned from Section III-A, the core component of the localization estimation is the per-antenna location probability estimation for each cell. That is, given the signal strength sample vector $S_i = [s_{i0}, s_{i1}, s_{i2}, ... s_{i\{n_i-1\}}]$ from antenna a_i where s_{ik} corresponds to angle $\theta_{ik} \in \Theta_i$, find the probability p_{ji} that the target is in cell c_j. In normal scenarios, it is possible to find an accurate estimator function of p_{ji} based on the pre-measured building knowledge such as WiFi fingerprint map or statistical RSSI-to-distance function curve-fitting. However, such parametric methods are not usable in limited scenarios where previous environment knowledge is unavailable or obsolete. Thus, any p_{ji} estimator function must rely on only spontaneous observation and non-parametric methods.

The section presents two non-parametric, heuristic-based p_{ji} estimator functions. The intuition of both functions is to estimate p_{ji} as the probability that cell c_j lies on the AoA between the device and the antenna a_i (i.e. calculate p_{ji} as $P[\theta(l_{a_i}, l_{c_j}) = \theta(l_{a_i}, l^*)|S_i]$). Both functions incur $O(1)$ computation delay per cell per antenna, resulting in $O(NM)$ delay for the whole localization process. The first function estimates the AoA probability of a cell based on pure RSSI values in S_i. The second function estimates the AoA probability of a cell based on non-parametric similarity between the measured signal distribution S_i and the antenna's ideal signal distribution, denoted by S_i^*.

1) RSSI-based Angle-of-arrival Probability Estimator: The basic intuition of this approach is that the stronger signal strength the target device receives from an antenna a_i at the AoA between a cell c_j and an antenna a_i, the more likely that the target is also in the same AoA as that cell c_j with respect to antenna a_i as well. Specifically, the RSSI-based AoA probability estimator of p_{ji} for cell c_j and antenna a_i is calculated as follows. First, the angle of arrival from antenna a_i to cell c_j, denoted by $\theta(l_{a_i}, l_{c_j})$, is calculated using Equation (2). Then the interpolated signal strength from antenna a_i to the target at the angle $\theta(l_{a_i}, l_{c_j})$, denoted by $s_i'(\theta(l_{a_i}, l_{c_j}))$ is calculated[1] from the signal vector S_i. Then, the probability p_{ji} is then calculated as

$$p_{ji} = P[\theta(l_{a_i}, l_{c_j}) = \theta(l_{a_i}, l^*)|S_i] \quad (3)$$

$$= \frac{s_i'(\theta(l_{a_i}, l_{c_j})) - \min(S_i)}{\max(S_i) - \min(S_i)} \quad (4)$$

[1]The interpolation can be done by linear weighted averaging of the signal samples from two angles in Θ_i that are adjacent to $\theta(l_{a_i}, l_{c_j})$

, where $\min(S_i)$ and $\max(S_i)$ are minimum signal value and maximum signal value in the vector S_i respectively.

That is, with this estimator, $p_{ji} = 0$ when $s'_i(\theta(l_{a_i}, l_{c_j})) = \min(S_i)$ and $p_{ji} = 1$ when $s'_i(\theta(l_{a_i}, l_{c_j})) = \max(S_i)$. Since $s'_i(\theta(l_{a_i}, l_{c_j}))$ is interpolated from S_i, the value of p_{ji} is always in [0,1] range. The probability p_{ji} is linearly proportional to the value of $s'(\theta(l_{a_i}, l_{c_j})) - \min(S_i)$.

Although the basic form of the RSSI-based AoA estimator has been previously explored [7], we include it in the framework for performance comparison. Furthermore, we propose in Section III-C a set of techniques which allow improvement over the basic RSSI-based estimator.

2) Correlative Ranking-based Angle-of-arrival Probability Estimator: The RSSI-based AoA probability estimator presented in Section III-B1 infers the target's AoA from the direction with the strongest RSSI. In reality, this may not be true due to signal reflection and attenuation. To reduce the effect of noise and attenuation, we propose the estimator that is based on *non-parametric similarity* between the measured signal angular distribution and the ideal signal angular distribution of the antenna. The ideal signal angular distribution of the antenna can be obtained from the antenna's specification or by direct measurement of the antenna's signal strength at close range and various angles in an open-space environment. Let $S^*_i(\theta)$ be the ideal RSSI from antenna a_i when measured at close range with the angle between a_i's beam and the receiver equal to θ. Given the ideal signal angular distribution $S^*_i(\theta)$ of a_i, we can estimate $P[\theta(l_{a_i}, l_{c_j}) = \theta(l_{a_i}, l^*)|S_i]$ by calculating how well the signal vector S_i, after being shifted by cell c_j's AoA $\theta(l_{a_i}, l_{c_j})$, aligns with $S^*_i(\theta)$. The process of shifting and checking alignment is as follows.

First, we define a θ-shifted sampling of antenna a_i's ideal signal, denoted by $S^{*\theta}_i$ as

$$S^{*\theta}_i = [s^{*\theta}_{i0}, s^{*\theta}_{i1}, s^{*\theta}_{i2}, ..., s^{*\theta}_{i\{n_i-1\}}]$$

, where $s^{*\theta}_{ik} = S^*_i(\theta_{ik} - \theta), \theta_{ik} \in \Theta_i$. Since the θ-shifted sampling $S^{*\theta}_i$ has the same dimension as S_i, the level of similarity between $S^{*\theta}_i$ and S_i can be used to determine the likelihood that AoA between the target and the antenna a_i is equal to θ (i.e. $P[\theta(l_{a_i}, l^*) = \theta|S_i]$). To compute the level of similarity between $S^{*\theta}_i$ and S_i, we use the non-parametric *Kendall Tau* rank correlation coefficient [10], which is used to measure the ranking similarity of two vectors. The Kendall Tau coefficient between $S_i = [s_{i0}, s_{i1}, ... s_{i\{n_i-1\}}]$ and $S^{*\theta}_i = [s^{*\theta}_{i0}, s^{*\theta}_{i1}, ..., s^{*\theta}_{i\{n_i-1\}}]$, denoted by $\tau_i(\theta)$, is calculated as

$$\tau_i(\theta) = \frac{\Sigma_{0 \le k < k' < n_i} I(k, k')}{\frac{1}{2} n_i (n_i - 1)}$$

, where

$$I(k, k') = \begin{cases} 1 & \text{if } \text{sign}(s_{ik'} - s_{ik}) = \text{sign}(s^{*\theta}_{ik'} - s^{*\theta}_{ik}) \\ -1 & \text{if } \text{sign}(s_{ik'} - s_{ik}) = -\text{sign}(s^{*\theta}_{ik'} - s^{*\theta}_{ik}) \\ 0 & \text{otherwise} \end{cases}$$

The function $\text{sign}(x)$ returns -1 if $x < 0$, returns 0 if $x = 0$ and returns 1 if $x > 0$. That is, $\tau_i(\theta)$ is the fraction of pair-wise rank matchings minus the fraction of pair-wise rank mis-matchings between S_i and $S^{*\theta}_i$. Hence, $\tau_i(\theta)$ will be equal to -1 if all pair-wise comparisons are mismatching and will be equal to 1 if all pair-wise comparisons are matching.

With the function $\tau_i(\theta)$ introduced above, the AoA probability p_{ji} can be calculated by first constructing $T_i = [\tau_i(\theta_{i0}), \tau_i(\theta_{i1}), \tau_i(\theta_{i2}), ..., \tau_i(\theta_{i\{n_i-1\}})]$, where each $\tau_i(\theta_{ik})$ represents the similarity of S_i and S^* when being shifted to $\theta_{ik} \in \Theta_i$. Then $\tau'_i(\theta(l_{a_i}, l_{c_j}))$ is linearly interpolated from T_i in the same way $s'_i(\theta(l_{a_i}, l_{c_j}))$ is interpolated from S_i in Section III-B1. Finally, p_{ji} is calculated in the same fashion as in Section III-B1. That is

$$p_{ji} = \frac{\tau'_i(\theta(l_{a_i}, l_{c_j})) - \min(T_i)}{\max(T_i) - \min(T_i)} \quad (5)$$

This correlative ranking-based AoA probability does not rely on the maximum RSSI, but uses overall measured RSSI distribution to calculate the AoA probability p_{ji} in a non-parametric style. Hence, it is more resilient to noise and attenuation than the RSSI-based estimator.

C. Accuracy-enhancing Techniques

While the two probability estimator functions presented Section III-B are suitable for our localization framework, their accuracy can be improved by various approaches that consider the antenna's physical characteristics. This section proposes three schemes to boost the accuracy of the estimators. The three schemes are the use of non-linear stretching, antenna beamwidth offset, and RSSI-distance upper bound.

1) Non-linear Stretching Parameter (K): The two estimators presented in Section III-B estimate cell c_j and antenna a_i AoA probability p_{ji} to be linearly proportional to the interpolated signal strength $s'_i(\theta(l_{a_i}, l_{c_j}))$ (or interpolated ranking coefficient $\tau'_i(\theta(l_{a_i}, l_{c_j}))$). However, this linear estimation may not be realistic to the physical characteristic of the antenna, where the probability increases non-linearly as the signal strength or ranking coefficient increases. To address this non-linear behavior, a simple adjustment is done as follows. Let p_{ji} be the estimated AoA probability from Equation (4) or Equation (5), we calculate a new probability with non-linear adjustment, denoted by p'_{ji}, as

$$p'_{ji} = 1 - (1 - p_{ji})^{\frac{1}{K}}$$

, where K is defined as *Non-linear Stretching Parameter* expressing how much the probability is distorted from linearity. The transformed probability p'_{ji} then replaces p_{ji} in the total cell probability calculation (Equation (1)).

Figure 2 shows the relationship between the original p_{ji} and the transformed p'_{ji} with different stretching factor K. The more K value is, the more bias towards high p_{ji} is. In the validation results in Section V, we will show that even though the setting of parameter K affects the accuracy of the localization, the effect is not high and hence the proposed schemes can work well over the wide range of K.

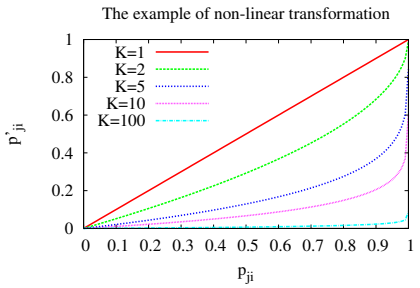

Figure 2. The non-linear transformation with different K

2) Non-zero Antenna Beamwidth Offset (B_i): Both probability estimator functions presented in Section III-B do not consider the antenna's non-zero beamwidth. Such non-zero beamwidth makes it hard to distinguish the antenna's AoA from other adjacent angles. This behavior is getting worse as the target's distance increases. To address the effect of the antenna's non-zero beamwidth, a modification is made at the calculation of interpolated signal strength $s'_i(\theta(l_{a_i}, l_{c_j}))$ in Section III-B1 (or cell interpolated ranking coefficient $\tau'_i(\theta(l_{a_i}, l_{c_j}))$ in Section III-B2) as follows.

$$s'_i(\theta(l_{a_i}, l_{c_j})) = \max_{\{k:|\theta_{ik}-\theta(l_{a_i},l_{c_j})|\leq\frac{B_i}{2}\}} s_{ik}$$

, where B_i is defined as the beamwidth offset of antenna a_i. That is, the interpolated signal strength $s'_i(\theta(l_{a_i}, l_{c_j}))$ is drawn from the maximum value $s_{ik} \in S_i$ that the corresponding angle $\theta_{ik} \in \Theta_i$ are within the $\frac{B_i}{2}$ degree from cell c_j's AoA angle $\theta(l_{a_i}, l_{c_j})$. Intuitively, this allows the probability estimator to calculate the probability based on the best value among the antenna's directions that are within the half beamwidth angle difference from $\theta(l_{a_i}, l_{c_j})$.

3) RSSI-distance upper bound: So far, the estimation of p_{ji} is calculated based on the AoA between cell c_j and antenna a_i without using any geographical distance between them. This is because the relationship between the RSSI and the distance in the building is considered as the environment information, which may be unavailable or obsolete at the time of the operation. However, while it is not possible to determine the exact RSSI-distance mapping, it is possible to determine the RSSI-distance *upper bound*. This is based on the observation that while it is generally possible for a receiver to get weak signal from an antenna despite short distance between them due to signal attenuation and reflection, it is rather unlikely for a receiver to get strong signal from the same antenna when they are far apart.

The RSSI-distance upper bound relationship can be obtained by measuring the RSSI at the receiver when facing to the antenna directly in open space at various distances. Figure 3 shows an example of RSSI-distance relationship of an antenna when measured in open space at the direct AoA. The power regression method is then used to estimate the function of such relationship. The estimated function is then used to provide the upper bound on the distance between the receiver and the antenna based on the RSSI.

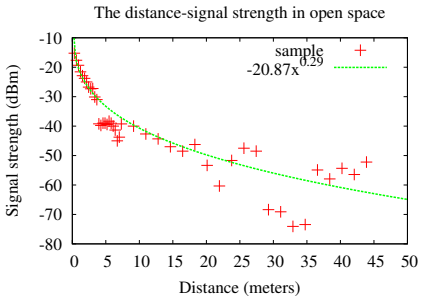

Figure 3. The distance-RSSI relationship in open space at the angle-of-arrival

Let $d^*(s)$ be the upper bound distance function of the received signal strength s (e.g. the inverse of the function in Figure 3). Hence, we add the filter at the last step of calculation of the probability p_{ji} from Equation (4) and Equation (5) as follows.

$$p'_{ji} = \begin{cases} p_{ji} & \text{if } D(l_{c_j}, l_{a_i}) \leq d^*(\max(S_i)) \\ 0 & \text{otherwise} \end{cases}$$

where $D(l_1, l_2)$ is the Euclidean distance between location l_1 and l_2. Hence, the cell c_j will be filtered out from the consideration if the distance between c_j and the antenna a_i is longer than the distance bound determined by the strongest signal strength in signal vector S_i.

IV. Antenna Scheduling Algorithms for Real-time Indoor Tracking

The previous section has described the localization algorithm for a static target where the target is able to receive signal from an antenna in every possible direction at the target's location. In reality, the target can be moving continuously and hence it is not possible to receive the signal readings from all available angles of each antenna all at once. Hence, in practice, the localization and tracking must be done based on partially stale scan samples. This section presents the antenna scheduling algorithm that determines the next scan direction of each antenna in order to locate a moving target with non-negligible signal reading delay.

We assume antenna a_i to continuously scan in various directions in its available direction set Θ_i. Each scan in a direction incurs delay d_i for each antenna a_i. Let θ_i^{curr} and θ_i^{next} be the current and next scan angles respectively. An antenna a_i must select the next scan direction θ_i^{next} after its current scan at direction θ_i^{curr} is finished. However, the control unit does not need to re-calculate the target's location every time an antenna finishes a scan in one direction to reduce overhead. Hence, we assume that the control unit localizes the target's current location every time period Δt using the most recent scan data S_i from each antenna a_i. This section presents two antenna scheduling algorithms: the static algorithm and the adaptive algorithm.

A. Static Antenna Scheduling Algorithm

When the localized target location feedback from the control unit to each antenna is not available, each antenna does not know which direction is the AoA from itself to the target. Hence, the best way to do the scanning is to give equal weight to each direction and scan each direction in a round robin style. That is,

$$\theta_i^{next} = \theta_{i\{(k+1) \bmod n_i\}}$$

when $\theta_i^{curr} = \theta_{ik}$.

B. Adaptive Antenna Scheduling Algorithm

If the localized target location feedback to antennas is available, then each antenna could do a more intelligent angle scheduling by scanning at the directions close to the target's AoA. For example, if an antenna knows that its AoA to the estimated current target position is 45^o, it is better to perform next scan at 45^o angle rather than at 70^o angle. However, scheduling an antenna based on only closeness to the feedback location may lead to inaccurate result as the antenna may never scan in some directions, resulting in very stale scan data. Hence, the adaptive antenna scheduling must take both target closeness and scan age into account as follows. Let $W_i = [w_{i0}, w_{i1}, ..., w_{i\{n_i-1\}}]$ be the weight for each possible scanning angle $\Theta_i = [\theta_{i0}, \theta_{i1}, ..., \theta_{i\{n_i-1\}}]$ of antenna a_i. Let $l^* = (x^*, y^*)$ be the target's estimated current position. Each angle's weight w_{ik} is calculated as

$$w_{ik} = \alpha_i.(1 - \frac{\theta_{ik}^{diff}}{360^o}) + (1 - \alpha_i)t_{ik} \quad (6)$$

, where t_{ik} denotes the elapsed time since antenna a_i's last scan at direction θ_{ik}, α_i denotes antenna a_i *weighting factor* to balance the weight between closeness to the target and the age of scan from each angle, and θ_{ik}^{diff} is the antenna a_i's angular difference between the angle θ_{ik} and the most recently estimated target's AoA. θ_{ik}^{diff} can be calculated as

$$\theta_{ik}^{diff} = \max[|\theta(l_{a_i}, l^*) - \theta_{ik}| - \arctan(\frac{\Delta t.V_{max}}{D(l_{a_i}, l^*)}) - \frac{B_i}{2}, 0]$$

where Δt is the elapsed time since last localization and $D(l_1, l_2)$ is the Euclidean distance between location l_1 and l_2. Intuitively, the angular difference θ_{ik}^{diff} considers time since last localization, target velocity bound V_{max}, and antenna beamwidth factor B_i.

Every time an antenna finishes its scan in one direction, the directional weight vector is updated using Equation (6). The direction with the highest weight is then scheduled as the next scan angle. The effect of different values of the weighting factor α_i will be shown in Section V-C.

V. Experimental Validation

In this section, we present the validation results of our proposed indoor localization and tracking algorithms with outdoor directional antennas. Section V-A describes the experimental setting in general. Section V-B presents the results of the proposed localization algorithm described in Section III. Finally, Section V-C shows the accuracy of the tracking algorithm presented in Section IV.

A. Experiment Settings

The specifications of hardware in our experiment are as follows. Each directional antenna is a Backfire 2.4 Ghz WiFi antenna from RadioLabs [11], which has 15 dB gain and 32^o half-power beamwidth. Each antenna is connected to a D-Link DI-524 wireless router [12]. Each pair of antenna and router is mounted to a manual tripod with 5^o angular scale marker. The example of one antenna is shown in Figure 4(b). All antennas obtain their geographic locations from landmark mapping using Google Maps service [9]. The antenna alignment is calibrated by an electronic compass. We use Nokia N95 phone with built-in 802.11g wireless interface as the target device in the experiment.

We conduct the experiment on a single-story house shown in Figure 4(a). The three star-shape points denote the deployment locations of three antennas. The other 21 circular points denote the placement of the target devices to collect the wireless radio signal inside the house. We deploy two antennas on the sidewalk outside the house and one antenna in the backyard. Each antenna is set up within a few minutes.

We divide the area into grid with cell size 0.1x0.1 meter^2 to balance the trade-off between accuracy and computation delay. The signal is collected from 21 points. Each directional antenna has the angle granularity of 5^o, which results in 72 directions (i.e., $\Theta_i = [0^o, 5^o, 10^o, ..., 350^o, 355^o]$ for all i). At each collection point, the wireless radio signal from each outdoor directional antenna is sampled in one complete round (72 readings from each antenna) with 15-second duration for each angle. Due to the device's reading delay, 15 seconds is the shortest time for the device to sense a change of signal level. In reality, we expect the reading delay to be much faster due to better hardware.

In Section V-B, the localization results at each of 21 collected points are shown. In Section V-C, the accuracy of the tracking algorithm is evaluated via simulations based on the trajectory shown in Figure 4(c). In the simulation, the RSSI at any point is linearly interpolated from the two closest collected sample points. As the distance between any two adjacent points in the trajectory is less than 3 meters, we believe that the interpolated RSSI is realistic enough to represent the real RSSI at any point in the trajectory.

B. Localization Accuracy

This section presents the accuracy of the localization algorithm based on real data collection previously described. We use the term '*rssi*' mode to refer to localization with the pure RSSI-based probability estimator (i.e. Section III-B1) and the term '*rank*' mode to refer to localization with the correlative ranking-based probability estimator (i.e. Section III-B2). Unless specifically stated, each localization result is done with 3 antennas, non-linear stretching parameter $K = 10$ and antenna beamwidth offset $B = 40^o$.

Angular Prediction Error: Figure 5(a) shows the distributions of angular errors of the two probability estimators.

(a) Experimental Map (b) Antenna Device (c) Simulated Target Trajectory

Figure 4. Experimental Settings

The angular error is the difference between the predicted AoA and the actual AoA from the target position to the antenna. The result shows that the ranking-based estimator is generally more accurate than the RSSI-based estimator (i.e. 5^o VS 10^o median error). Note that more than 80% of errors are within half of the antenna's half-power beamwidth (i.e., 16^o), indicating that the AoA prediction from both estimators are good with respect to the hardware capability.

Positioning Error: Figure 5(b) presents the distribution of positioning errors in meters of the two probability estimators, with and without the RSSI-distance bound (from Section III-C3). The results indicate that the rank-based estimator performs slightly better than the rssi-based estimator. Also, the use of RSSI-distance bound noticeably improve the accuracy of the two estimators by more than 50%.

RSSI-distance Bound: To validate the correctness of the RSSI-distance bound, Figure 5(c) shows the relationship between the distance from each sample point to each anchor, and the corresponding RSSI from the strongest direction. The bound line is the distance upper bound (or RSSI lower bound) estimation from Figure 3. The results show that around 90% of the points are within the estimated bound. Only 10% of the points receive stronger signal than the bound. One explanation is that these points are focal points where signal from multiple directions accumulate, resulting in stronger signal than usual. A better bound for such uncommon corner cases is left as future work.

Effect of Beamwidth Offset Parameter (B_i): As described in Section III-C2, the beamwidth offset parameter B_i for each antenna a_i can be used to reduce the positioning error caused by the antenna's half-power beamwidth. Figure 5(d) shows the average positioning errors of the two estimators, with and without distance bound, for different values of the beamwidth offset parameter B_i. Since all 3 antennas are of the same model, we use the same B_i for all antennas. The results show that the optimal B_i value is around $25^o - 35^o$, which is consistent to the 33^o half-power beamwidth from the antenna's specification. Hence, we conclude that B_i parameter for antenna a_i can be set to the half-power beamwidth specification of the antenna a_i for good accuracy.

Effect of Non-linear Stretching Parameter (K): Figure 5(e) presents the average localization errors with different non-linear stretching parameter values (K) proposed in Section III-C1. The results show that the localization performs better as K grows larger, with the optimal $K = 20$. This validates the hypothesis that the AoA-based probability is not linearly proportional to RSSI value nor RSSI ranking. Note that when $K = 1$, the RSSI-based estimator without RSSI-distance bound exactly represents the work of Niculescu and Nath [7], which gives the average error of 4.07 meters in our experiment. By using the ranking-based estimator with RSSI-distance bound and a proper value of K, we can reduce the average error down to 2.56 meters.

Effect of Additional Antennas : Figure (5(f)) shows the localization error distributions of the ranking-based estimator with RSSI-distance bound when using 2 anchors (i.e., the two leftmost anchors in Figure 4(a)) and 3 anchors (i.e., all anchors in Figure 4(a)). The result shows that the accuracy slightly improves when the number of anchors increases from 2 to 3. Due to time and resource limitation, we do not experiment with more anchors. However, we expect the number of anchors to be less than 4 or 5 due to the quick set-up time requirement. The question of how to find the best locations to deploy each antenna is left as future work.

C. Tracking Accuracy

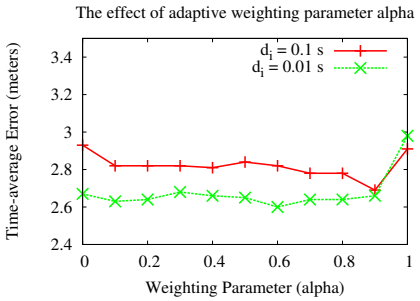

Figure 7. The tracking accuracy under different $alpha$

This section presents the simulation results of the static and adaptive antenna scheduling algorithms for real-time indoor tracking proposed in Section IV. In the simulations, the target is simulated to move with the trajectory shown in Figure 4(c) at 1 m/s maximum speed. We test the scheduling algorithms with 3 antennas and 3 signal reading delay d_i values (1s, 0.1s, 0.01s). The tracking period T is set to 1

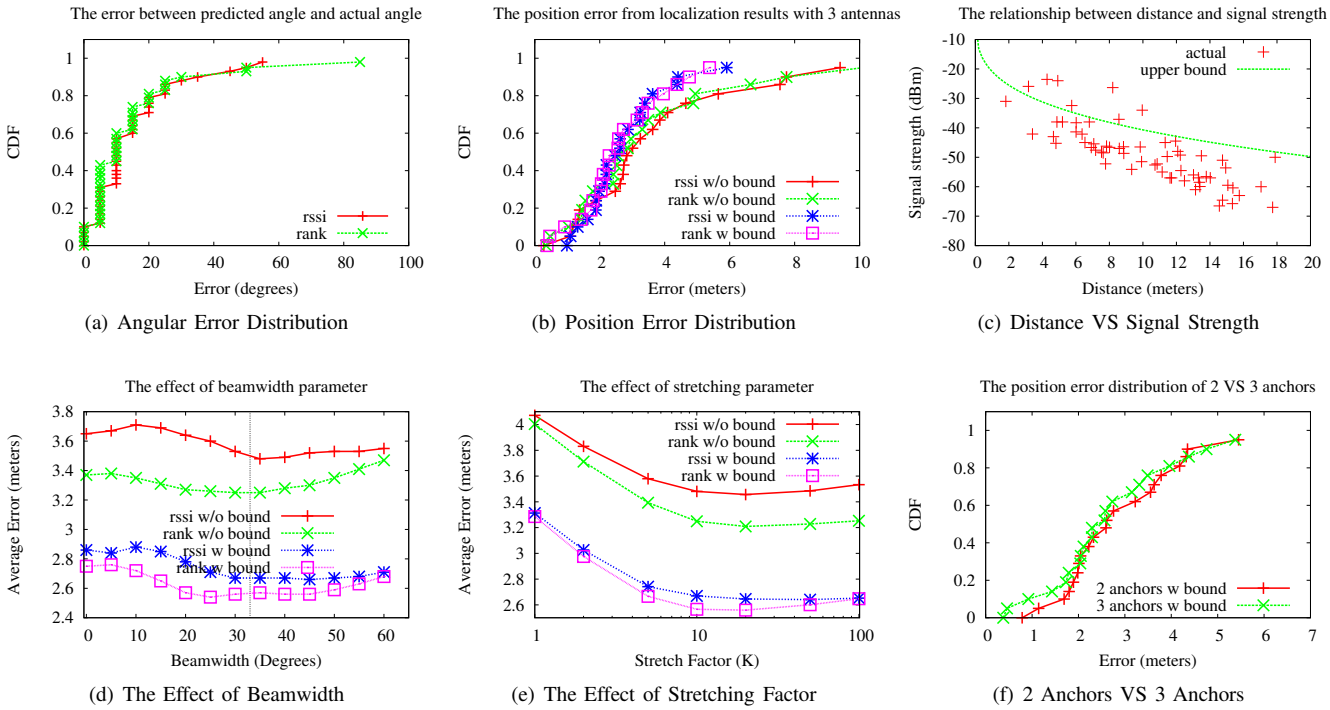

(a) Angular Error Distribution (b) Position Error Distribution (c) Distance VS Signal Strength

(d) The Effect of Beamwidth (e) The Effect of Stretching Factor (f) 2 Anchors VS 3 Anchors

Figure 5. Localization Accuracy

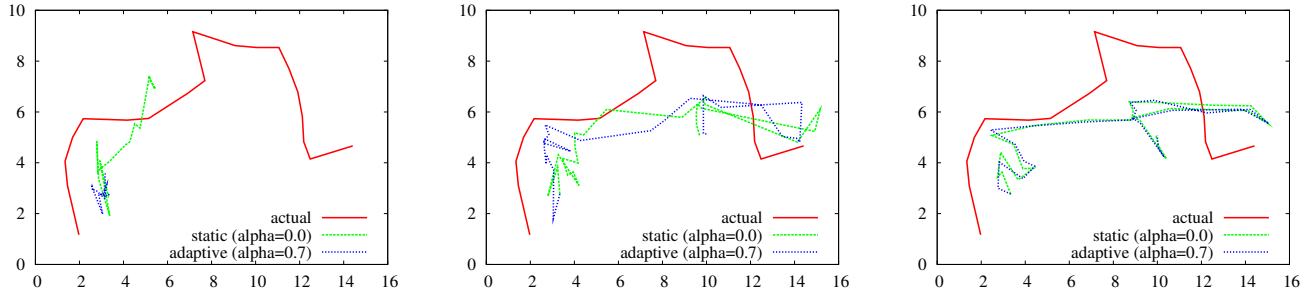

(a) d_i=1s (b) d_i=0.1s (c) d_i=0.01s

Figure 6. Tracking Trajectory with Different Latency

second, which means the target is localized every second with the most recent scanning data from each antenna.

Figure 6 shows the trajectory of the tracking algorithm under 3 different signal reading delay d_i. From the results, we can draw the following conclusions. First, the tracking result diverges from the correct trajectory if the antenna's scanning speed is too low. Second, the more scanning speed the antenna has, the more accurate the tracking result is. Finally, the adaptive scheduling only improves the accuracy when the antenna's scanning speed is not too high and not too low (i.e. Figure 6(b)). The reason is if the antenna's speed is too low, the estimated position is totally different from the actual position, giving the adaptive scheduler false feedback. However, if the antenna scanning speed is too high, the scanning order then becomes less significant.

Figure 7 shows the effect of the weighting factor α to the average tracking accuracy. Note that the tracking algorithm is static if $\alpha = 0$ and adaptive otherwise. The graph shows that the accuracy of the tracking is better when α is more than 0.0, which means that the adaptive scheduling is better than the static scheduling. However, the tracking accuracy gets worse when $\alpha = 1$ since the algorithm does not take the angle's age into account at all, leading to very stale reading in some angles. Also, the effect of α has less impact when $d_i = 0.01$ second, as compared to when $d_i = 0.1$ second. This confirms the assumption that adaptive scheduling is less

beneficial under high antenna scanning speed.

VI. Related Works

This section discusses the works related to this paper in two areas: WiFi-based indoor localization, and indoor tracking in emergency scenarios.

A. WiFi-based Indoor Localization

Works on WiFi-based indoor localization can be divided into two categories. The first category localizes targets by using the received signal strength indicator (RSSI) from omni-directional antennas to determine the target's position [1], [2]. This class of localization algorithms assume a mapping between RSSI and spatial metrics (e.g., relative distance or absolute position). To get accurate results, such mapping must be pre-calculated specifically for each building, which is unsuitable for emergency scenarios.

Another category of WiFi-based localization techniques is to estimate the angle-of-arrival (AoA) and distance from directional antennas to the target location [6]–[8]. Most of works in this category assume several directional antennas placed *inside* the building to localize a *static* indoor object. We believe our paper is the first work to use few *outdoor* directional antennas to track a *moving* indoor target.

B. Indoor Tracking in Emergency Scenarios

Many indoor tracking schemes for emergency scenarios have been proposed so far [4], [5], [13]–[16]. Overall, there are three approaches for tracking target inside buildings. The first approach, a scattered sensor-based technique, pre-deploys sensors equipped with wireless devices such as RFID and WiFi inside buildings [13], [14]. Although this technique can be used to collect other information than signal strength (i.e., temperature), it is expensive and sometimes not possible to deploy many sensors beforehand.

On the other hand, the second approach, called dead reckoning [4], [15], exploits inertial sensors and pedometers carried by the targets to estimate moving distance and directions. The accuracy of this approach depends on the accuracy of the inertial sensors. This approach is orthogonal to our work and the combination of both works is possible.

In the third approach, a small number of base stations which emit beacons are set outside the building. Our work is categorized in this approach. However, our work is the first work to use WiFi directional antenna to track the target. Other candidates include UWB and omni-directional WiFi [5], [16], which usually assume the environment knowledge of the building such as signal fingerprint or per-building signal-distance mapping. Our approach does not assume such knowledge to be known prior to the operation.

VII. Conclusions

This paper has presented a set of indoor localization and tracking algorithms to track an indoor moving object by a small set of outdoor directional antennas. First, the paper presented the probabilistic, grid-based localization framework to calculate the location probability of a static target based on per-antenna AoA probability estimator. The paper then presented two non-parametric AoA probability estimators to be used in the framework. The paper then discussed the antenna scheduling algorithms based on the proposed localization algorithm to track an indoor moving target. Finally, the paper presented the validation results based on real data collection and simulations. The results have shown that the proposed schemes achieve good accuracy despite the use of off-the-shelf hardware in the implementation. We believe this work would open a new possibility for WiFi-based object tracking in emergency scenarios.

References

[1] P. Bahl and V. N. Padmanabhan, "Radar: an in-building rf-based user location and tracking system," in *Proc. INFOCOM'00*, vol. 2, 2000, pp. 775–784.

[2] M. B. Kjærgaard and C. V. Munk, "Hyperbolic location fingerprinting: A calibration-free solution for handling differences in signal strength," in *Proc. PerCom'08*, 2008, pp. 110–116.

[3] M. Azizyan, I. Constandache, and R. Roy Choudhury, "Surroundsense: mobile phone localization via ambience fingerprinting," in *Proc. MobiCom'09*, 2009, pp. 261–272.

[4] J. Guerrieri, M. Francis, P. Wilson, T. Kos, L. Miller, N. Bryner, D. Stroup, and L. Klein-Berndt, "Rfid-assisted indoor localization and communication for first responders," in *Proc. EuCAP'06*, 2006, pp. 1–6.

[5] D. Dardari, A. Conti, J. Lien, and M. Z. Win, "The effect of cooperation on localization systems using uwb experimental data," *EURASIP J. Adv. Signal Process*, vol. 8, no. 2, pp. 1–11, 2008.

[6] A. P. Subramanian, P. Deshpande, J. Gao, and S. R. Das, "Drive-by localization of roadside wifi networks," in *Proc. INFOCOM'08*, 2008, pp. 718–725.

[7] D. Niculescu and B. Nath, "Vor base stations for indoor 802.11 positioning," in *Proc. MobiCom '04*, 2004, pp. 58–69.

[8] E. Elnahrawy, J.-A. Francisco, and R. P. Martin, "Bayesian localization in wireless networks using angle of arrival," in *Proc. SenSys'05*, 2005, pp. 272–273.

[9] "Google maps," http://maps.google.com.

[10] M. Kendall, "A new measure of rank correlation," *Biometrika*, vol. 30, pp. 81–89, 1938.

[11] "Radiolabs antennas," http://www.radiolabs.com.

[12] "D-link wireless routers," http://www.dlink.com.

[13] J. Wilson, V. Bhargava, A. Redfern, and P. Wright, "A wireless sensor network and incident command interface for urban firefighting," in *Proc. MobiQuitous'07*, 2007, pp. 1–7.

[14] V. Kumar, D. Rus, and S. Singh, "Robot and sensor networks for first responders," *IEEE Pervasive Computing*, vol. 3, no. 4, pp. 24–33, 2004.

[15] J. Saarinen, S. Heikkila, M. Elomaa, J. Suomela, and A. Halme, "Rescue personnel localization system," *Proc. SSRR'05*, pp. 218–223, June 2005.

[16] N. Alsindi and K. Pahlavan, "Cooperative localization bounds for indoor ultra-wideband wireless sensor networks," *EURASIP J. Adv. Signal Process*, vol. 8, no. 2, pp. 1–13, 2008.